

*Biochimica et Biophysica Acta*, 513 (1978) 117–131

© Elsevier/North-Holland Biomedical Press

BBA 78181

## INTERACTION OF *PSEUDOMONAS* CYTOCHROME $cd_1$ WITH THE CYTOPLASMIC MEMBRANE

MATTI SARASTE and TAPANI KURONEN

*Department of Medical Chemistry, University of Helsinki, Siltavuorenpenger 10, SF-00170 Helsinki 17 and Central Public Health Laboratory, SF-00280 Helsinki 28 (Finland)*

(Received January 10th, 1978)

### Summary

Labelling with ferritin-conjugated antibody shows that *Pseudomonas* cytochrome  $cd_1$  is associated with the inner surface of the cytoplasmic membrane. Cytochrome  $cd_1$  is, however, enriched to the soluble fraction obtained after destruction of *Pseudomonas* spheroplasts. Comparison of the respiratory nitrite reductase activities, due to this cytochrome, between different cellular fractions and the purified enzyme shows that while the kinetic pattern and the temperature dependence of the activity remain almost the same the molecular activity is enhanced when the enzyme is released from cells.

A new assay of respiratory nitrite reductase was developed in this study. The method is based on determination of the stoichiometrical proton consumption accompanying nitrite reduction.

---

### Introduction

The respiratory enzymes in the bacterial cell, or in the mitochondrion, are incorporated into membranous structures which are essential in coupling of respiratory activities to oxidative phosphorylation, active transport, and related energy-requiring phenomena [1]. Some of these enzymes are lipoprotein complexes integrally constructed in the membrane bilayer, while some are associated more loosely, peripherally, with membranes. For example, many bacterial dehydrogenases and *c*-type cytochromes fall in the latter category [2].

*Pseudomonas* cytochrome oxidase (cytochrome *c*-551:  $O_2$ ,  $NO_2^-$  oxidoreductase, EC 1.9.3.2), which is a cytochrome  $cd_1$ , can be extracted from acetone-dried [3] or mechanically destructed [4] bacterial cells without the aid of

---

Abbreviations: TMPD, *N,N,N',N'*-tetramethyl-*p*-phenyldiamine; EDTA, ethylenediaminetetraacetic acid; HEPES, *N*-2-hydroxyethylpiperazine-*N'*-ethanesulphonate.

detergents. The purified enzyme is composed of two identical monomers [5,6] and is soluble in buffer solutions.

The properties of the purified enzyme have been investigated in many laboratories (see refs. 3–7). It is therefore interesting to re-investigate the enzymic properties of this cytochrome *in situ*, and to compare them with the previous results. The study reported in this communication has been aimed at elucidating two aspects of the enzyme in the bacterial cell: (i) the localization of the enzyme in the cell, and (ii) comparison of the functional characteristics of the enzyme *in situ* with those of the purified enzyme.

In a previous study we suggested that the interaction between the dimeric enzyme and a liposomic membrane is essentially extrinsic. However, the enzyme is attached to the reconstituted membrane in a way which affects the catalytic activity [8]. In this context it is interesting to find out whether a similar effect on the enzymic activity results from interaction with the cytoplasmic membrane.

In this paper we report that *Pseudomonas* cytochrome *cd*<sub>1</sub> is associated with the inner surface of the cytoplasmic membrane. Some quantitative differences are found between the enzymic properties of the purified and membrane-attached cytochromes. However, the similarities in kinetic parameters indicate that the purified enzyme is functionally very similar to the enzyme in the cell.

## Materials and Methods

*Pseudomonas* cytochrome *cd*<sub>1</sub> was purified as previously reported [5]. Cytochrome *c*-551 and azurin were purified by the method of Ambler [9]. Lysozyme was purchased from Nutritional Biochemicals Corp. (Cleveland, Ohio), DNAase (DN-25) from Sigma and twice-crystallized horse spleen ferritin as a 10% solution from Serva. Glutaraldehyde, specially purified for electron microscopy, was obtained from Taab Laboratories and *N,N,N',N'*-tetramethyl-*p*-phenyldiamine hydrochloride (TMPD) from Fluka. The other reagents used were of the highest purity class available commercially.

### *Cultivation of bacterial cells and preparation of spheroplasts and membrane vesicles*

*Pseudomonas aeruginosa* (the strain of bacteria was the same as previously used [5]) was grown in a citrate-yeast extract medium containing 0.5% (w/v) sodium nitrite [5]. The cells were cultivated for 6 h at 30°C in 2-l Erlenmeyer flasks containing 1 l of the medium. The cultures were stirred continuously by means of a magnetic flea. The cells were harvested by centrifugation at 4°C for 15 min at 10 000 × *g*.

Spheroplast formation of these cells, collected in the middle of the log phase, was induced by the lysozyme-EDTA treatment [10]. Two modifications of the method, described by Osborn and Munson [11] and Witholt et al. [12], gave essentially similar results. In both cases, the procedure led to an uncontrolled lysis of the osmotically sensitized cells \*. Subsequently, DNAase was

---

\* In this paper we have adapted Kaback's [10] nomenclature for the manipulated bacterial cells.

added to lower the viscosity of cell suspensions. The spheroplasts were collected by centrifugation for 15 min at  $2000 \times g$ .

For preparation of the membrane vesicles, the spheroplast suspension was ultrasonicated after the lysozyme-EDTA treatment in 20-ml batches with a Branson Sonifier B-12 (Branson Power Co, Danbury, Conn.) operated at 50 W. Sonication was carried out 3 times for 15 s in an ice-bath. The undisrupted cells were removed by centrifugation for 15 min at  $2000 \times g$ , whereafter the membrane vesicles were pelleted (45 min at  $82000 \times g$ ) and suspended in 10 mM Tris (pH 7.8)/20 mM KCl/2 mM  $MgCl_2$ . This pelleted material will be referred to below as the "membrane vesicles" (see Fig. 5), and the supernatant fraction obtained as the "supernatant".

#### *Preparation of ferritin-conjugated antibody to cytochrome $cd_1$*

An antiserum was prepared by immunizing a rabbit with purified cytochrome  $cd_1$ . The animal was subcutaneously injected into the hind foot twice with 1 mg of the protein emulsified in complete Freund's adjuvant and once with 2 mg protein without the adjuvant. The injections and the bleeding were done fortnightly. Immunoglobulin G fraction was separated from the serum by precipitation with 40% saturated ammonium sulphate and by chromatography in a DEAE-cellulose column [13] in 20 mM potassium phosphate buffer (pH 6.5). The first elution peak ( $A_{280\text{nm}}$ ) was used as the anticytochrome  $cd_1$ . Mono-specificity and antigenicity of the immunoglobulin fraction is shown in Fig. 1, A and B. Only one precipitation line was observed against crude extracts of *Pseudomonas* cells and no precipitation against cytochrome c-551 and azurin. The maximal inhibition of nitrite reductase activity (see below) by the antibody was approx. 80%.

The anticytochrome  $cd_1$  was linked to ferritin with glutaraldehyde by the modified two-stage method [14]. The dialyzed ferritin was first activated with 0.1% (w/v) glutaraldehyde for 40 min at  $37^\circ\text{C}$ , and the activated ferritin was separated from unreacted glutaraldehyde in a Sephadex G-25 column. In the second stage the anticytochrome  $cd_1$ , at final concentration 3 mg/ml, was

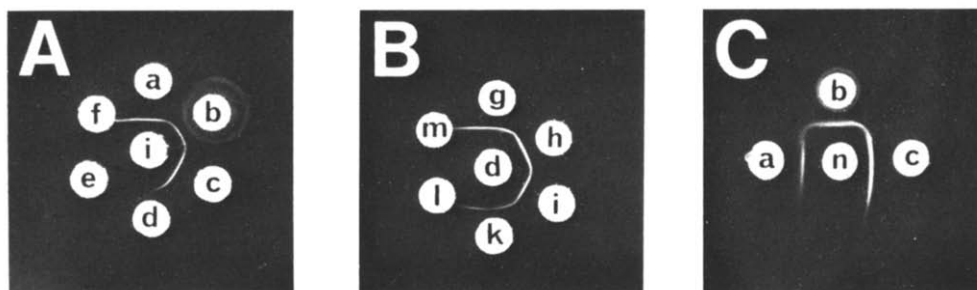


Fig. 1. Antigenicity of anticytochrome  $cd_1$  and anticytochrome-ferritin conjugate. The figures A, B and C show unstained double immunodiffusion patterns in 1.5% (w/v) purified agar gels buffered with 50 mM Tris-HCl (pH 7.9). Each well contained 10  $\mu\text{l}$  of following samples. A: (a), cell-free extract of acetone-dried *Pseudomonas* cells (7 mg protein/ml); (b), extract made with 3% (w/v) Triton X-100 from the bacterial cells (10 mg/ml); (c), cytochrome  $cd_1$  (0.26 mg/ml); (d), cytochrome  $cd_1$  (0.09 mg/ml); (e), azurin (1.3 mg/ml); (f), cytochrome c-551 (3.7 mg/ml); central well (i), anticytochrome  $cd_1$  (0.63 mg/ml). B: (g–m), 2-fold dilutions of anticytochrome  $cd_1$ . C: (a–c), the same samples as in A; central well (n), ferritin-anticytochrome  $cd_1$  conjugate.

allowed to react with the activated ferritin (9 mg/ml) for 24 h at 37°C. Concentration determinations of activated ferritin were based on the absorption coefficient at 440 nm  $A_{1\text{ cm}}^{1\%} = 15.4$ . Ferritin-anticytochrome  $cd_1$  conjugate was further purified from high molecular weight aggregates, free ferritin and immunoglobulin by gel chromatography in a Sepharose 4 B column (Fig. 2). Fractions 48–52 were concentrated 30-fold with Minicon B 15 (Amicon N.V.). After testing for antigenicity (Fig. 1C) the concentrate was used as the immunoferritin label. The antigenicity of the immunoglobulin was not changed during the conjugation (compare Fig. 1, A, B and C).

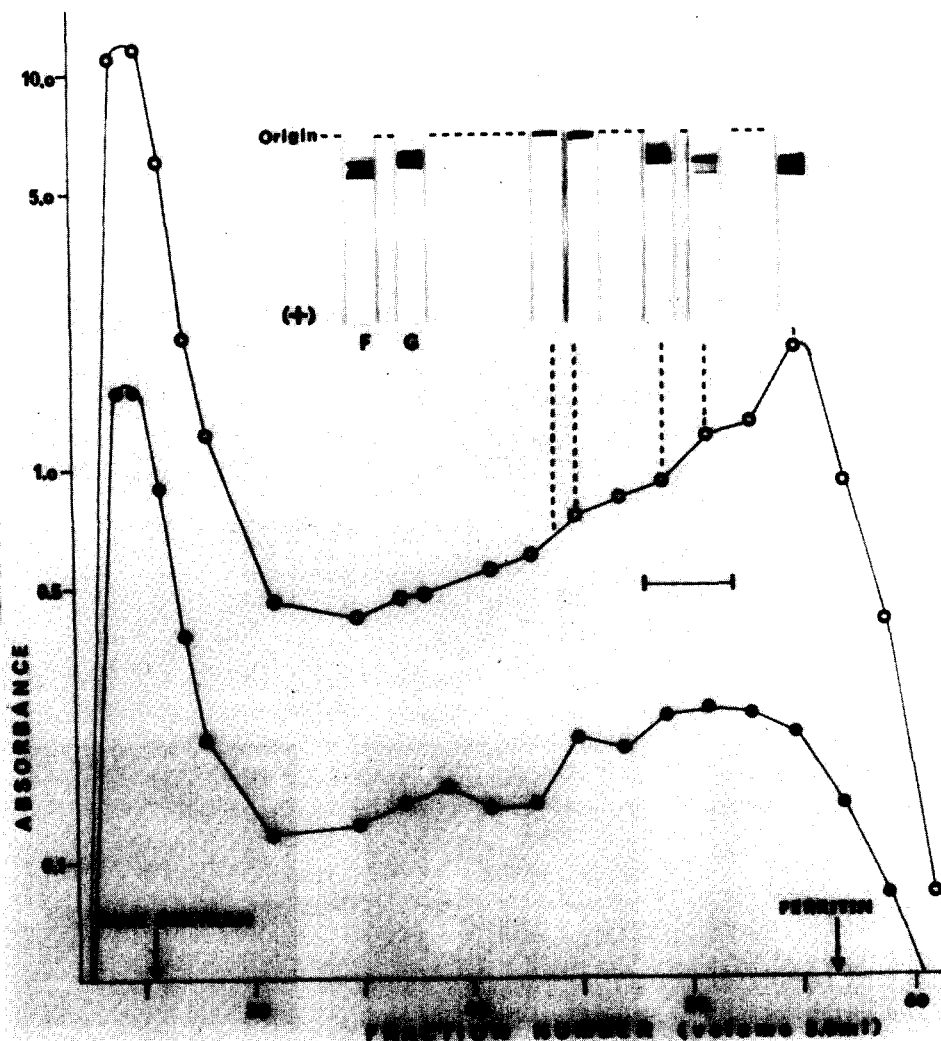
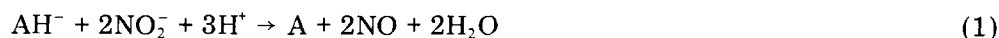


Fig. 2. Gel chromatography of ferritin-anticytochrome  $cd_1$  conjugate. Gel chromatography of the ferritin-anticytochrome  $cd_1$  conjugate was carried out in a Sepharose 4 B columns (2.5 × 46 cm), which was equilibrated with 0.1 M sodium phosphate (pH 7.4) and precalibrated with Blue Dextran and ferritin (arrows). The fractions were analyzed by the absorbance at 280 nm (○—○) and at 440 nm (●—●). The bar marks the fraction chosen for immuno-ferritin labelling. Electrophoresis of the fractions was performed in 7% (w/v) polyacrylamide gels. The electrophoretic patterns of ferritin (F) and anticytochrome  $cd_1$  (G) are shown for comparison.

**Electron microscopy.** The bacterial samples were labelled with the ferritin-conjugated antibody by mixing 25  $\mu$ l label with 200  $\mu$ l spheroplast or membrane vesicle suspension (10 mg protein/ml) and incubating the suspension for 5–15 h at 4°C. The samples were pelleted, washed with Tris buffer and processed for electron microscopy. Prefixation was carried out in 3% (v/v) glutaraldehyde for 3 h at 0°C. Postfixation in 1% (w/v) OsO<sub>4</sub>, thin-sectioning and staining with lead citrate and uranyl acetate were carried out conventionally. The thin sections were examined with a JEM 100 B (Jeol) electron microscope.

#### *Determination of nitrite reductase activity*

The nitrite reductase activity was measured indirectly with a pH electrode. Nitrite consumption was determined from the rate of proton consumption according to the following reaction (where A denotes ascorbate):



i.e. ,

$$\Delta[\text{NO}_2^-] = 0.67\Delta[\text{H}^+] .$$

Ascorbate, which was used as reductant, is partially deprotonated at pH 7 ( $pK_1$  4.14 for ascorbic acid). TMPD served as redox mediator between ascorbate and the cytochrome system. Nitric oxide has been reported to be the end product of the reaction catalyzed by the purified cytochrome *cd*<sub>1</sub> [15,16].

An Ingold combination electrode (W. Ingold, Zürich) was fitted to a thermostated anaerobic cuvette, which was constantly fluxed with nitrogen. The reaction was carried out in nitrogen-saturated 0.5 mM *N*-2-hydroxyethylpiperazine-*N'*-ethanesulphonate (HEPES) buffer (pH 6.90)/150 mM KCl/2 mM MgCl<sub>2</sub>. Ascorbate (3.3 mM), TMPD (0.05 mM) and the sample were added in 3.0 ml buffer, and the reaction was started by addition of 10  $\mu$ l 1 M sodium nitrite. When the buffer was completely free of dissolved oxygen, no alkalization was observed upon the addition of ascorbate and TMPD. In the presence of oxygen autooxidation of ascorbate occurred with consequent proton consumption.

The nitrite reductase activity was determined from the initial slopes of proton consumption read out on a strip-chart recorder. In this phase, the other proton-consuming reactions (e.g. reduction of nitric oxide or hydroxylation of dehydroascorbate, see ref. 17 for the latter reaction) are certainly absent. Addition of cyanide (1 mM) completely inhibited the proton consumption.

#### *Other determinations*

Protein was determined by the biuret method [18] with bovine serum albumin as standard.

The heme *d*<sub>1</sub> content of the preparations was measured from the absorbance of the pyridine hemochromogen formed in alkaline solution. The samples were solubilized into 0.25 M NaOH/pyridine (2 : 1), and a few grains of sodium dithionite were added. After standing for 10 min, the spectra were scanned between 550 and 700 nm with an Aminco DW-2 spectrophotometer. The difference of absorbances at 618 and 670 nm, ( $A_{618-670\text{ nm}}$ ) was determined to be

$23.6 \text{ mM}^{-1} \cdot \text{cm}^{-1}$  using the purified cytochrome  $cd_1$  as standard (1 mol heme  $d_1$ /63 000 g protein [5,6]).

## Results

### *Absorption spectrum of the Pseudomonas cells*

The reduced minus oxidized difference spectrum of the *P. aeruginosa* cells, recorded at the temperature of liquid nitrogen, shows the presence of *b*-type (spectral bands at 527 and 556 nm), *c*-type (513, 521, 548 and 552 nm), and *d*-type (600–650 nm) cytochromes (curve 1 in Fig. 3). When the cells are destructed by sonication and the membrane vesicles are separated from the soluble material, the *b*-type cytochromes are retained in the vesicle fraction. A rather great part of the *c*-type cytochromes and the *d*-type cytochromes are almost exclusively recovered in the soluble fraction (see curves 2 and 3 in Fig. 3). There is no cytochrome *d* in the bacterial cells (which should retain in

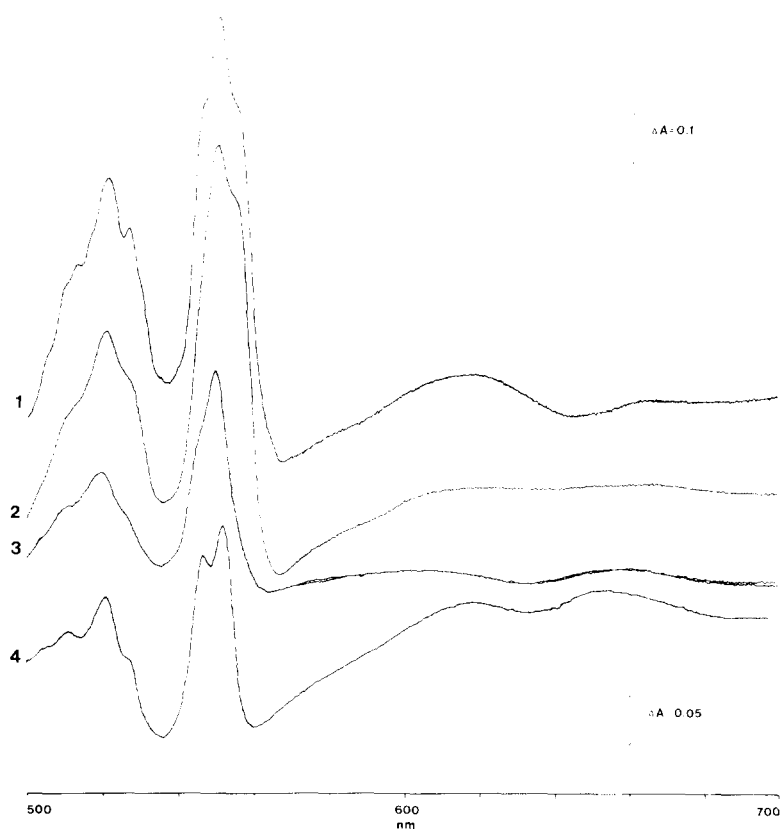


Fig. 3. Absorption spectrum of *Pseudomonas* cells and cellular subfractions. The log-phase cells (curve 1), membrane vesicles and soluble fraction (curve 3) were prepared as described in Materials and Methods. The difference spectra (reduced with dithionate minus oxidized with ferricyanide) were recorded at 77 K from 500 to 700 nm. Light path of the cuvette was 0.2 cm. The difference spectrum of the purified cytochrome  $cd_1$  is shown for comparison (curve 4). The protein concentrations were 8.0, 8.0, 2.8 and 2.1 mg/ml in 1, 2, 3 and 4, respectively. The absorbancy scale  $\Delta A = 0.1$  for the curve 1 and  $\Delta A = 0.05$  for the other curves is indicated in the upper and lower right corners, respectively.

membrane vesicles) but the 600–650 nm spectrum is due to the cytochrome  $cd_1$  (crude 4 in Fig. 3 presents the spectrum of the purified cytochrome  $cd_1$  for comparison).

The cytochrome  $cd_1$  is not, however, the only cytochrome oxidase in the semi-aerobically cultivated cells. Membrane vesicles which had the highly reduced content of heme  $d_1$  contained a remarkable cytochrome oxidase activity. When ascorbate and TMPD were used as the electron donating system [8], the polarographically determined rate of oxygen consumption in the bacterial cell suspension was  $0.102 \mu\text{mol O}_2/\text{min}$  per mg protein and in the membrane vesicle suspension  $0.163 \mu\text{mol O}_2/\text{min}$  per mg. Approximately 58% of the oxidase units were recovered in the membrane vesicles. This cytochrome oxidase activity is probably due to a cytochrome “o”-type enzyme, because no cytochrome  $a_1$ , which has been reported to be present in aerobically cultivated *P. aeruginosa* [19], was found under the conditions of growth used in this study.

#### *Assay of nitrite reductase*

All determinations of enzymic activity of cytochrome  $cd_1$  were carried out measuring reduction of nitrite. Respiratory nitrite reductase is supposed to involve only cytochrome  $cd_1$  in *Pseudomonas* cells. The nitrite reductase assay developed in this study excludes interferences from a possible assimilatory enzyme, which requires NADH or NADPH as the electron donor [20,21]. When nitrite reductase activity of the bacterial cells was determined, the cell suspension was preincubated aerobically to exhaust the endogenous substrates.

The stoichiometry between nitrite and proton consumption in reaction (1), which was used in the activity calculations, was confirmed experimentally both with the purified enzyme and with the bacterial cells (Table I, A and B, respectively). At the initial phase of the reaction the stoichiometry of consumed protons to nitrite was found to be 1.5 within the experimental error. The same stoichiometry was also found in determinations of the total amount of protons consumed after additions of small, defined amounts of nitrite when the reaction was catalyzed by the purified enzyme (Table I, A). In contrast, the consumed protons to nitrite ratio tended to rise when the reaction went further in bacterial cell suspension (Table I, B). The total amount of protons was consumed after additions of nitrite far exceeded the 1.5 stoichiometry and even the expected amount of protons was consumed upon denitrification of the added nitrite to nitrogen (which should be 2.5 if ascorbate can donate all the reducing equivalents in analogy to reaction (1)). However, the nitrite reductase activities were determined from the initial slope of the reaction, and the apparent absence of proton consuming “side-reactions” during the initial reaction phase shows that the indirect nitrite reductase assay can be used also for activity determinations with bacterial cells, or with the subsequently obtained cellular fractions.

#### *Association of cytochrome $cd_1$ with the cytoplasmic membrane*

A typical electron micrograph of *Pseudomonas* spheroplasts is shown in Fig. 4a. Together with cytoplasmic vesicles which still contain part of the

TABLE I

## STOICHIOMETRY OF NITRITE AND PROTON CONSUMPTION IN THE NITRITE REDUCTASE ASSAY

The activity measurements were performed at 21.5°C, as described in Materials and Methods, with purified cytochrome *cd*<sub>1</sub> (24 µg) in A, and *Pseudomonas* cells (480 µg protein) in B. Reaction was stopped by addition of potassium cyanide (1.7 mM), and the residual nitrite determined according to ref. 22. The initial nitrite concentration was 0.10 mM. Total proton consumption caused by a defined amount of nitrite (45 and 50 nmol in A and B, respectively) is also included in the Table.

	Time (sec)	NO <sub>2</sub> <sup>-</sup> consumed (nmol)	H <sup>+</sup> consumed (nmol)	$\frac{\Delta [H^+]}{\Delta [NO_2^-]}$
A.	17	19	27	1.42
	30	26	39	1.50
	40	31	47	1.52
	95	50	69	1.38
	150	66	99	1.51
Total reaction		45	68	1.51
B.	18	5	7	1.4
	35	7	12	1.7
	55	12	19	1.58
	70	16	26	1.62
	89	19	36	1.89
	160	32	71	2.21
Total reaction		50	460	9.20

cytoplasmic constituents of the cell (spheroplasts), and small outer membrane vesicles formed in the lysozyme-EDTA treatment, a few cell ghosts are observable. These are usually double-membrane vesicles retaining both cytoplasmic and outer membranes. In the thin-sectioned preparations the outer membranes are revealed by their distinct trilaminar structure [23].

When the type of preparation shown in Fig. 4a is labelled with the ferritin-conjugated antibody to cytochrome *cd*<sub>1</sub>, the label is rarely observed to be associated to the outer surface of the cytoplasmic membrane, which is potentially subjected to labelling after destruction of the outer membrane and the peptidoglycan layer. In the spheroplast preparations the label is attached on the inner surface of the cell ghosts (Fig. 4, b and c) or to the inside of unsealed and partially plasmolyzed cells (Fig. 4d) occasionally seen in the micrographs. Membranes of the cell ghosts are likely to retain their original orientation in the intact cell, and the membrane surface which is labelled in Fig. 4, b and c, should be the inner surface of the cytoplasmic membrane.

Even membrane vesicles with a reduced content of the antigen, which is solubilized during ultrasonic destruction of the spheroplasts, are labelled with the ferritin-conjugated antibody (Fig. 5). Some of the label seen in these preparations is not bound to the membranous vesicles but is attached to material without any resolved structure. Most of the membrane vesicles bind the ferritin-antibody, which would indicate a prominent inside-out orientation of the cytoplasmic membrane vesicles after sonication. No labelling of membrane vesicles or spheroplasts prepared from *nir*-mutants of *P. aeruginosa* (generous gift of Dr. J. van Hartingsveldt), which have no nitrite reductase activity and no heme *d*<sub>1</sub> spectrum [24], was observed in experiments parallel to those shown in Figs. 5 and 6 (data not shown).



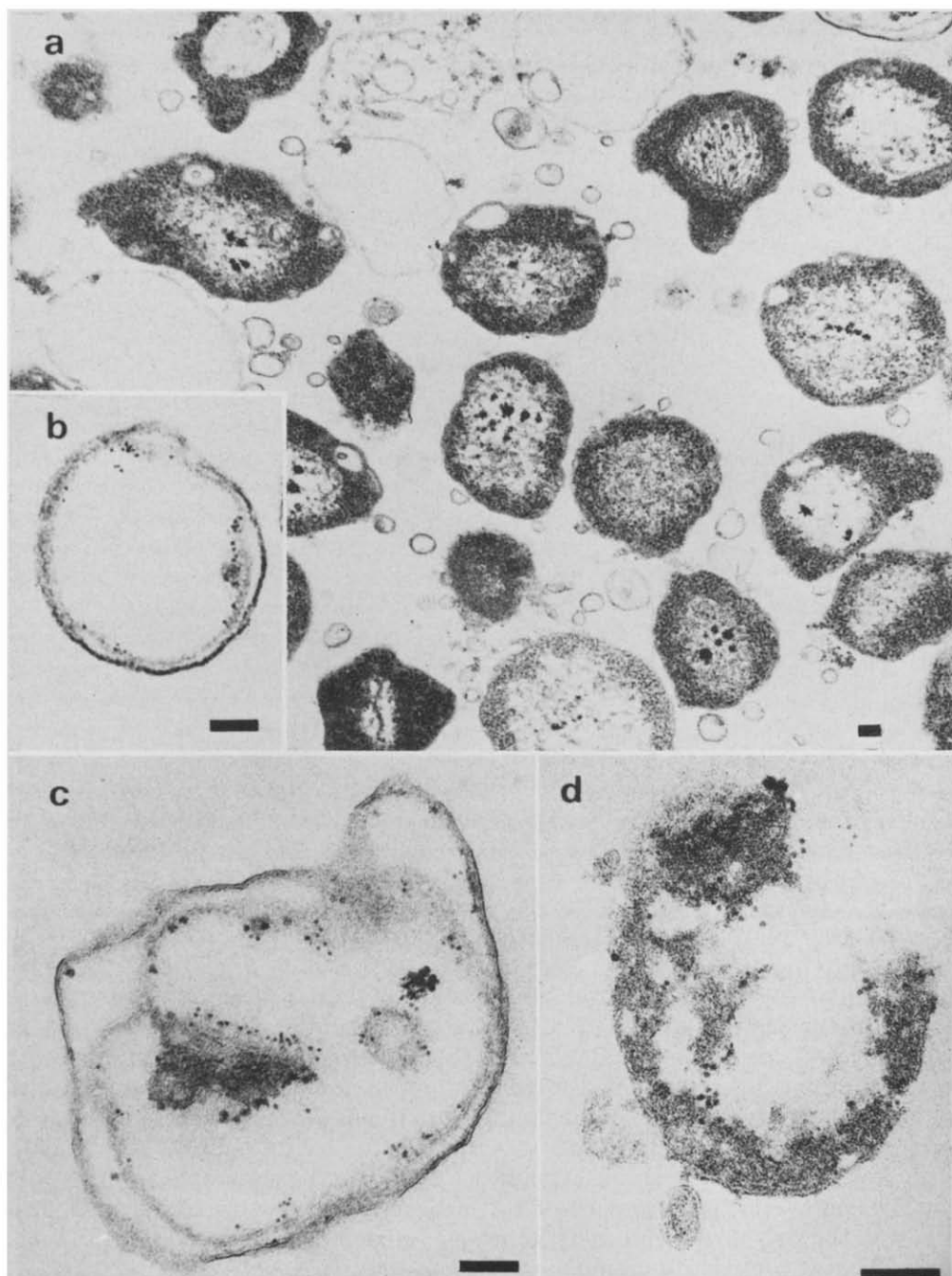


**Fig. 4.** Labelling of *Pseudomonas* spheroplasts with ferritin-conjugated antibody to cytochrome *cd*<sub>1</sub>. (a) Spheroplasts of *P. aeruginosa* prepared by the lysozyme-EDTA method [10,11] and labelled with the ferritin-antibody (see Materials and Methods); (b) and (c), cell ghosts labelled with the ferritin-antibody; (d), a fragment of the bacterial cell labelled with the ferritin-antibody. Magnifications are 30 000, 60 000, 80 000, and 90 000  $\times$  diameters in a, b, c, and d, respectively. The bars represent 100 nm. See text for further explanation.

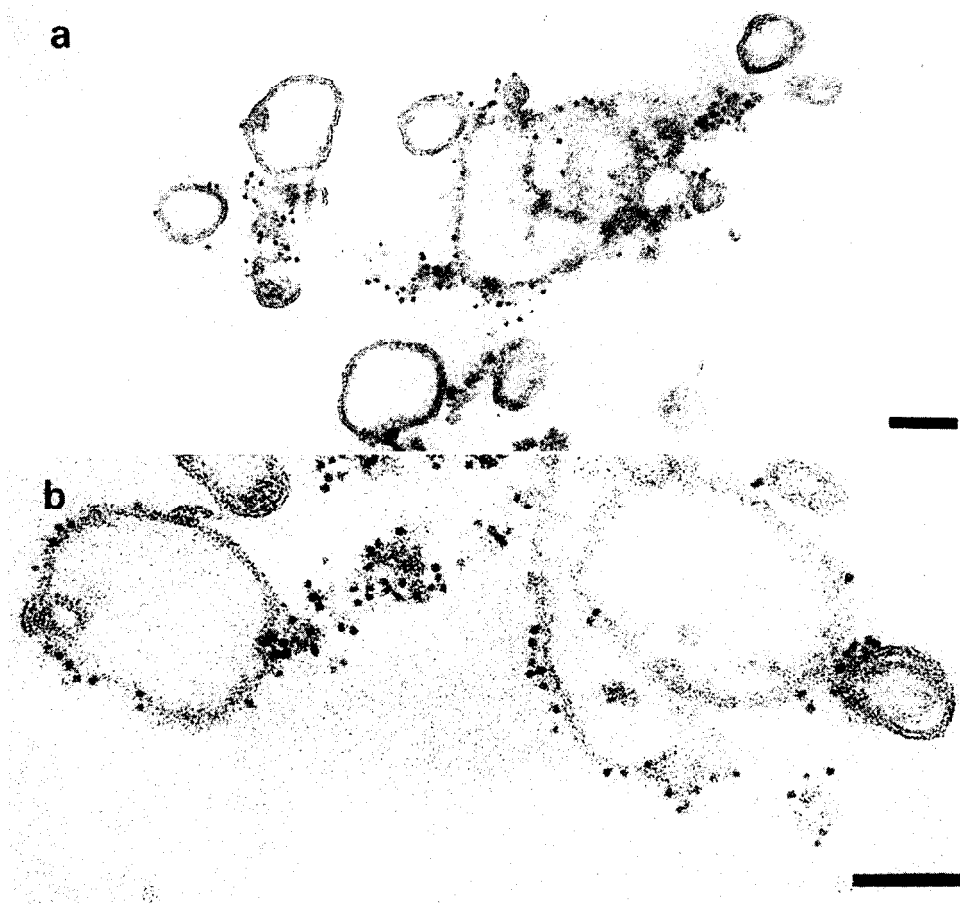


Fig. 5. Membrane vesicles labelled with ferritin-conjugated antibody to cytochrome  $cd_1$ . Membrane vesicles were prepared as described and labelled with the ferritin-antibody (see Materials and Methods). Magnifications are 90 000 and 150 000  $\times$  diameters in (a) and (b), respectively. The bars represent 100 nm.

The lines of evidence above, obtained from the labelling studies, indicate that cytochrome  $cd_1$  is located inside the cytoplasmic membrane, and that at least a part of the enzyme is attached to the inner surface of the membrane.

All the previous studies on the purification of the enzyme have shown that it is rather easily released from the bacterial cells (see e.g. ref. 4). This was confirmed in this study. The specific activity of the nitrite reductase is enriched into the supernatant fraction after destruction of the spheroplasts (Tables II and III). However, the presence of the antigen for the ferritin-conjugated antibody in the cell ghosts and membrane vesicles demonstrate that the enzyme is associated with the cytoplasmic membrane *in situ*.

#### *Comparison of enzymic activities*

The effect of "solubilization" of the nitrite reductase was studied by measuring the molecular activities, the apparent Michaelis constants, and activation energies of nitrite reduction in different cellular fractions, and comparing them with the properties of the purified enzyme.

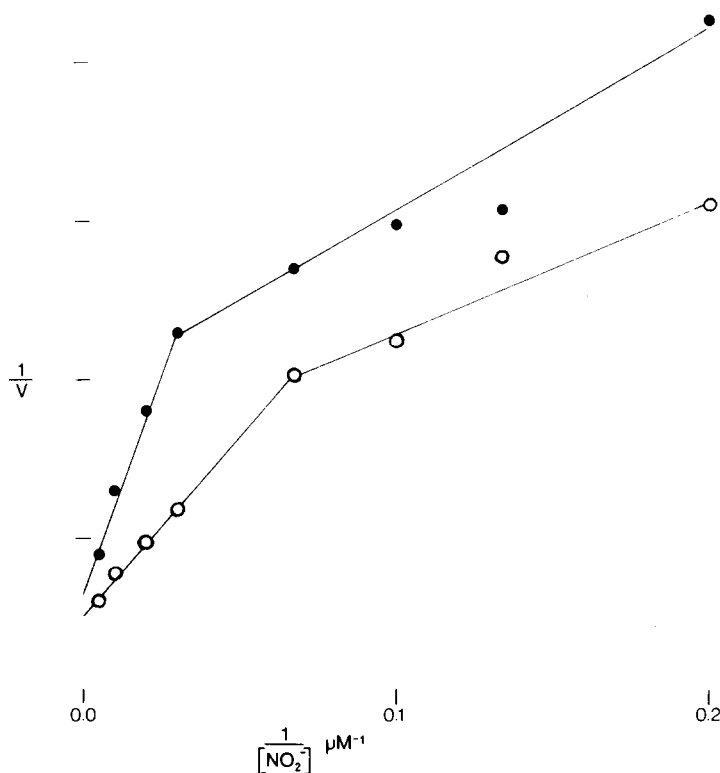


Fig. 6. Affinity of *Pseudomonas* cytochrome  $cd_1$  to nitrite. Lineweaver-Burk plots were calculated from the initial velocities of nitrite reduction in different sodium nitrite concentrations (from 5 to 200  $\mu M$ ). The nitrite reductase activity was determined as described in Materials and Methods with bacterial cells (●—●, 420  $\mu g$  protein in the assay) or purified cytochrome  $cd_1$  (○—○, 57  $\mu g$  protein in the assay). The points were calculated from the means of two parallel determinations, and tentatively resolved in a biphasic manner (solid lines). The ordinate is in arbitrary units.

TABLE II

#### NITRITE REDUCTASE ACTIVITIES IN DIFFERENT CELLULAR FRACTIONS

The bacterial cells were converted to spheroplasts by the lysozyme-EDTA method, and these were lysed by ultrasonication. 'Membrane vesicles' refers to the pelleted material and 'supernatant' refers to the soluble fraction obtained after destruction of the spheroplasts. The enzymic activity (five parallel determinations, S.D. indicated) and the heme  $d_1$  content (the means of two parallel determinations) were measured as described in Materials and Methods. The heme  $d_1$  content of the purified enzyme was calculated on the base of the minimal molecular weight [5,6].

Preparation	Heme $d_1$ content ( $\mu mol/g$ protein)	Specific activity ( $\mu mol NO_2^-/min$ per mg)	Molecular activity ( $mol NO_2^-/min$ per $mol$ heme $d_1$ )
Bacterial cells	0.183	$0.099 \pm 0.006$	$541 \pm 33$
Membrane vesicles	—	$0.017 \pm 0.002$	—
Supernatant	0.272	$0.201 \pm 0.039$	$736 \pm 143$
Purified enzyme	15.87	$20.90 \pm 0.29$	$1315 \pm 38$

TABLE III

## RECOVERY OF NITRITE REDUCTASE IN DIFFERENT CELLULAR FRACTIONS

The different preparations are described in the legend to Table II. 'Undestructed cells' refers to the fraction pelleted at  $2000 \times g$  after the sonic treatment of the spheroplasts. The initial amount of bacterial cells were obtained from 1 l of medium after 7 h of cultivation. The unit of activity is  $\mu\text{mol NO}_2^-/\text{min per mg protein}$ .

Preparation	Total protein		Heme $d_1$ content		Specific activity	
	mg	%	nmol	%	Units	%
Bacterial cells	422	100	77.2	100	41.8	100
Understructed cells	97	30.0	15.7	20.3	8.6	20.6
Membrane vesicles	117	27.7	—	—	2.0	4.6
Supernatant	205	48.6	55.8	72.3	41.2	98.6
$\Sigma$		99.3		92.4		124.0

Molecular activity tends to rise when the enzyme is extracted from the cell and further isolated from the other cellular components (Table II). (Molecular activity in the membrane vesicle fraction could not be measured due to low heme  $d_1$  content in it.) The activation is also seen when recovery of the nitrite reductase units is calculated: the units are enriched into the supernatant (Table III). Increase in the total nitrite reductase units upon the purification of the enzyme has also been reported earlier [25].

The apparent Michaelis constants for nitrite are, in contrast, rather similar for the enzyme in the intact cell, in the extract and in purified form (Table IV). Lineweaver-Burk analysis of the data reveals complicated kinetics of biphasic character shown in Fig. 6. In any case it is obvious that the kinetics are very similar in the bacterial cells, in the supernatant fraction (not shown in Fig. 6) and in the purified preparation. The "low-affinity" constants are of the same order of magnitude as previously obtained ( $53 \mu\text{M}$ , ref. 15).

The changes in activation energies of nitrite reduction (see Table IV and Fig. 7) are consistent with the changes in molecular activities: when the latter rises, the former is lowered. It is remarkable that temperature dependence of the activity in the cells fits very well to a straight line ( $r^2 = 0.99$  in Fig. 7, A and B).

TABLE IV

## KINETIC PARAMETERS OF NITRITE REDUCTASE IN DIFFERENT CELLULAR FRACTIONS

The apparent Michaelis constants were determined from the Lineweaver-Burk plots (see Fig. 6). (a) and (b) refer to the apparent 'high-affinity' and 'low-affinity' constants resolved from the plots. The activation energies were calculated from activity measurements in the temperature range  $4-45^\circ\text{C}$  (Fig. 7). Data of the supernatant, which refers to the soluble fraction obtained after sonication, are not included in Figs. 6 and 7.

Preparation	Apparent $K_m$ for $\text{NO}_2^-$ ( $\mu\text{M}$ )		Activation energy (kcal/mol)
	(a)	(b)	
Bacterial cells	6.2	84.5	9.98
Supernatant	6.1	49.5	8.63
Purified enzyme	5.3	48.0	7.84

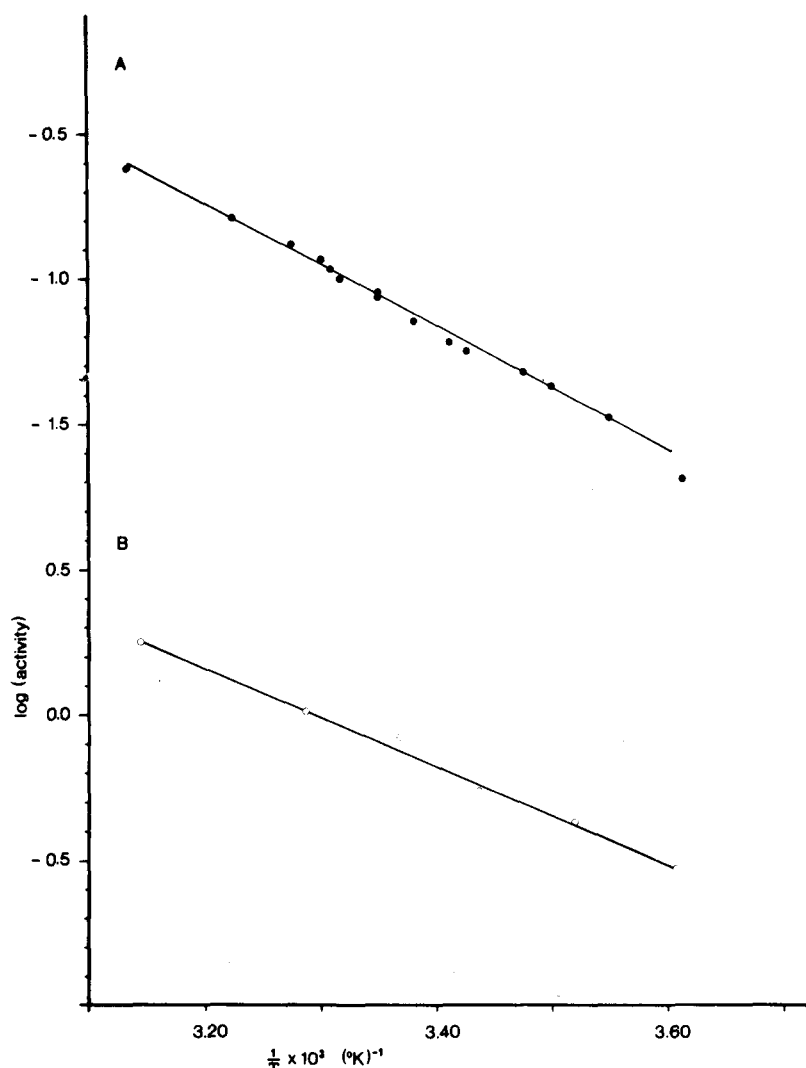


Fig. 7. Temperature-dependence of the nitrite reductase activity. The Arrhenius plots were calculated from the means of three parallel determinations of maximal velocities of nitrite reduction at temperatures ranging from 4 to 45°C. The activity was calculated as  $\mu\text{mol NO}_2^-/\text{min}$ . A and B represent the temperature-dependence of the activity in bacterial cells (480  $\mu\text{g}$  protein in the assay) and of the purified cytochrome  $cd_1$  (57  $\mu\text{g}$  protein in the assay), respectively. The lines were calculated by linear regression.

## Discussion

Our results show that the cytochrome  $cd_1$  is located on the inner surface of the cytoplasmic membrane in the *Pseudomonas* cell. This leaves two possibilities. The enzyme may be quantitatively bound to the membrane in situ, and is largely dissociated from it during manipulation of the bacterial cells. Alternatively, there exists an equilibrium between the membrane-attached and cytoplasmic forms of the enzyme. Both possibilities involve an interaction between the enzyme and the cytoplasmic membrane, which, as we have shown, affects enzymic activity.

Walker and Nicholas [25] interpreted the increase of nitrite reductase units upon purification of the enzyme to be due to separation of an inhibitor from the enzyme. It is also possible that activation of the enzyme is due to its release from the membranous structures, and to changes in its quaternary structure upon solubilization (for instance, dimerization of the monomeric enzyme). It is not clear whether this would have any physiological significance.

The Arrhenius plot of the nitrite reductase activity in intact cells fits well with a straight line (Fig. 7A). This suggests that changes in the physical state of the membrane phospholipids do not influence the nitrite reductase activity. Such an interaction should be revealed by non-linearities in the Arrhenius plot (see refs. 26–28). Linearity in the plot would correspond to extrinsic location of a membrane-bound enzyme.

The biphasic kinetics observed in Lineweaver-Burk plots (Fig. 6) cannot be easily interpreted at present. Possible explanations are the presence of two isoenzymes with different affinities to nitrite, or an equilibrium between dimeric and monomeric forms of the enzyme, or interaction of the two  $\text{NO}_2^-$ -binding sites in the dimeric enzyme. Whatever the correct interpretation is, it is clear the enzyme kinetics are similar *in situ* and in the purified state.

We have tried to determine the effect of uncouplers of oxidative phosphorylation on the nitrite reductase activity in the bacterial cells. So far no stimulation of the activity (measured as described in Materials and Methods) has been observed. It should be noted that nitrite itself may act as an uncoupler, because it can symport protons through the membrane [29]. It is obvious from the results of this communication, and from the previous data [6,8], that the cytochrome *cd*<sub>1</sub> molecule per se is certainly not transmembranous. It is presently widely accepted that energy-transducing redox-enzyme complexes catalyze transmembrane proton flux (see refs. 30–32 for recent reviews). However, the enzyme might yet form part of a coupling site through interaction with other membrane proteins.

The coupling of nitrite reductase in denitrifying bacteria with oxidative phosphorylation has not yet been clearly solved [31,32] while the nitrite-reducing electron transfer (denitrification) can, of course, support cellular life [33]. More topological and bioenergetic studies are needed to resolve the coupling sites in denitrifying bacteria. The site of nitrite reduction in *Pseudomonas* cells seems to be located on the inner surface of the cytoplasmic membrane.

## Acknowledgements

The nitrite reductase assay was suggested by Dr. John Ingledew. We thank Dr. Mårten Wikström for criticism during preparation of the manuscript, and Mrs. Sirkka Rönholm for typewriting. The excellent technical assistance of Inari Arponen and Ulla Piililä is gratefully acknowledged.

## References

- 1 Mitchell, P. (1966) *Chemiosmotic Coupling in Oxidative and Photosynthetic Phosphorylation*, Glynn Research, Bodmin

- 2 Gel'man, N.S., Lukoyanova, M.A. and Ostrovskii, D.N. (1975) *Bacterial Membranes and the Respiratory Chain. Biomembranes*, (Manson, L.A., ed.), Vol. 6, Plenum Press, New York
- 3 Horio, T., Higashi, T., Yamanaka, T., Matsubara, H. and Okunuki, K. (1961) *J. Biol. Chem.* 236, 944—951
- 4 Parr, S.R., Barber, D. and Greenwood, C. (1976) *Biochem. J.* 157, 423—430
- 5 Kuronen, T. and Ellfolk, N. (1972) *Biochim. Biophys. Acta* 275, 308—318
- 6 Kuronen, T., Saraste, M. and Ellfolk, N. (1975) *Biochim. Biophys. Acta* 393, 48—54
- 7 Gudat, J.C., Singh, J. and Wharton, D.C. (1973) *Biochim. Biophys. Acta* 292, 376—390
- 8 Saraste, M. (1978) *Biochim. Biophys. Acta*, 507, 17—25
- 9 Ambler, R.P. (1963) *Biochem. J.* 89, 341—349
- 10 Kaback, H.R. (1971) *Methods Enzymol.* 22, 99—120
- 11 Osborn, R.M. and Munson, R. (1974) *Methods Enzymol.* 31, 642—653
- 12 Witholt, B., Boekhout, M., Brock, M., Kingma, J., van Heerikhuizen, H. and de Leij, L. (1976) *Anal. Biochem.* 74, 160—170
- 13 Livingston, D.M. (1975) *Methods Enzymol.* 34 B, 723—731
- 14 Otto, H., Takamiya, H. and Vogt, A. (1973) *J. Immunol. Methods* 3, 137—146
- 15 Yamanaka, T., Ota, A. and Okunuki, K. (1961) *Biochim. Biophys. Acta* 53, 294—308
- 16 Shimada, H. and Orii, Y. (1975) *FEBS Lett.* 54, 237—240
- 17 Hinkle, P.C. (1973) *Fed. Proc.* 32, 1973—1992
- 18 Gornell, A.G., Bardawell, C.J. and David, M.M. (1949) *J. Biol. Chem.* 177, 751—766
- 19 Azouley, E. (1964) *Biochim. Biophys. Acta* 92, 458—464
- 20 Nason, A. (1962) *Bacteriol. Rev.* 26, 16—41
- 21 Kemp, J.D. and Atkinson, D.E. (1966) *J. Bacteriol.* 92, 628—634
- 22 Losada, M. and Peneque, A. (1971) *Methods Enzymol.* 23, 487—491
- 23 Nakamura, K. and Mizushima, S. (1975) *Biochim. Biophys. Acta* 413, 371—393
- 24 Van Hartingsveldt, J. and Stouthamer, A.H. (1973) *J. Gen. Microbiol.* 74, 97—106
- 25 Walker, G.C. and Nicholas, D.J.D. (1961) *Biochim. Biophys. Acta* 49, 350—360
- 26 Davis, D.G., Inesi, G. and Gulik-Krzywicki, T. (1976) *Biochemistry* 15, 1271—1276
- 27 Boldyrev, A., Ruuge, E., Smirnova, I. and Tabak, M. (1977) *FEBS Lett.* 80, 303—307
- 28 Bäter, A.J. and Venables, W.A. (1977) *Biochim. Biophys. Acta* 468, 209—226
- 29 Purczeld, P., Chon, C.J., Portis, Jr., A.R., Heldt, H.W. and Heber, U. (1978) *Biochim. Biophys. Acta* 501, 488—498
- 30 Harold, R.M. (1977) in *Current Topics in Bioenergetics* (Rao Sanadi, D., ed.), Vol. 6, pp. 84—149, Academic Press, New York
- 31 Haddock, B.A. and Jones, C.W. (1977) *Bacteriol. Rev.* 41, 47—99
- 32 Thauer, R.K., Jungermann, K. and Decker, K. (1977) *Bacteriol. Rev.* 41, 100—180
- 33 van Verseveld, H.W., Meijer, E.M. and Stouthamer, A.H. (1977) *Arch. Microbiol.* 112, 17—23